Modeling carbon export mediated by biofouled microplastics in the Mediterranean Sea

Federica Guerrini [ORCID],[1,2*] Delphine Lobelle [ORCID],[2] Lorenzo Mari [ORCID],[1] Renato Casagrandi [ORCID],[1*]
Erik van Sebille [ORCID][2,3]
[1]Department of Electronics, Information, and Bioengineering, Politecnico di Milano, Milan, Italy
[2]Institute for Marine and Atmospheric Research, Utrecht University, Utrecht, The Netherlands
[3]Centre for Complex Systems Studies, Utrecht University, Utrecht, The Netherlands

Abstract

Marine microplastics can be colonized by biofouling microbial organisms, leading to a decrease in microplastics' buoyancy. The sinking of biofouled microplastics could therefore represent a novel carbon export pathway within the ocean carbon cycle. Here, we model how microplastics are biofouled by diatoms, their consequent vertical motion due to buoyancy changes, and the interactions between particle-attached diatoms and carbon pools within the water column. We initialize our Lagrangian framework with biogeochemical data from NEMO-MEDUSA-2.0 and estimate the amount of organic carbon exported below 100 m depth starting from different surface concentrations of 1-mm microplastics. We focus on the Mediterranean Sea that is characterized by some of the world's highest microplastics concentrations and is a hotspot for biogeochemical changes induced by rising atmospheric carbon dioxide levels. Our results show that the carbon export caused by sinking biofouled microplastics is proportional to the concentration of microplastics in the sea surface layer, at least at modeled concentrations. We estimate that, while current concentrations of microplastics can modify the natural biological carbon export by < 1%, future concentrations projected under business-as-usual pollution scenarios may lead to carbon exports up to 5% larger than the baseline (1998–2012) by 2050. Areas characterized by high primary productivity, that is, the Western and Central Mediterranean, are those where microplastics-mediated carbon export results to be the highest. While highlighting the potential and quantitatively limited occurrence of this phenomenon in the Mediterranean Sea, our results call for further investigation of a microplastics-related carbon export pathway in the global ocean.

The mechanisms regulating the carbon cycle in the ocean are being increasingly perturbed by global changes triggered by increasing greenhouse gas emissions caused by anthropogenic activities (Wanninkhof et al. 2013) and by the manifold feedback mechanisms consequently triggered (Heinze et al. 2019). The so-called *global biological carbon pump* is a pathway linking the relatively fast air–sea interactions with the slower deep geological carbon cycle (Falkowski et al. 2003) that is expected to be impacted by changes in nutrient availability, rising temperatures, and increasing atmospheric carbon dioxide concentrations (Laufkötter et al. 2016; The Intergovernmental Panel on Climate Change [IPCC] 2021, 2022). Climatologists are currently unable to precisely predict the extent of these modifications (Passow and Carlson 2012); in terms, both of their intensity and the marine areas involved. In fact, simultaneous changes in the carbonate system, temperature, vertical mixing, and nutrient regimes of the pelagic environment are expected to manifest differently in distinct regions of the ocean (McGinty et al. 2011). In particular, the Mediterranean Sea is known for being one of the regions that is most sensitive to global change (Giorgi 2006) as well as a mesocosm that foreshadows ongoing alterations of marine ecosystems worldwide (Lejeusne et al. 2010).

Similarly to ongoing trends in the global ocean, the rich Mediterranean biodiversity (about 7% of the world's marine

*Correspondence: federica.guerrini@polimi.it; renato.casagrandi@polimi.it

Additional Supporting Information may be found in the online version of this article.

biodiversity; Coll et al. 2010) is also being severely impacted by other types of human interference (Micheli et al. 2013), including plastic pollution. A recent study by Everaert et al. (2020) highlighted that, in 2010, 15.9% of the Mediterranean surface was characterized by concentrations of microplastics exceeding the predicted no-effect concentration (a threshold for toxicity) for several species, with even more unfavorable projections in business as usual future scenarios. Marine productivity is consequently expected to be impacted by microplastic pollution (Troost et al. 2018), with reductions in phytoplankton photosynthesis and growth (Sjollema et al. 2016; Tetu et al. 2019), and in the development and reproduction of zooplankton (Cole et al. 2015), all of which are key regulating mechanisms of the biological carbon pump. For example, ingested microplastics can change the density and sinking rates of zooplankton fecal pellets (Cole et al. 2016), also modifying the remineralization rates and the aggregation/disaggregation of the particulates that constitute the majority of the carbon flux to depth (Chen et al. 2018; Porter et al. 2018), including marine snow (Kharbush et al. 2020). When incorporated into other components of the marine biological pump, such as marine snow and sinking of zooplankton fecal pellets, microplastics could slow down the carbon export related to them (Long et al. 2015; Cole et al. 2016; Wieczorek et al. 2019).

In addition to manifesting changes in marine productivity due to microplastic pollution, the mechanisms described above may additionally transport significant amounts of microplastics to depth (Kvale et al. 2020*a,b*), hinting to the fate of the "missing" fraction of surface microplastics (Cózar et al. 2014; Eriksen et al. 2014; Van Sebille et al. 2015), together with particle sinking caused by biofouling (Egger et al. 2020; Nguyen et al. 2020; Van Melkebeke et al. 2020). A variety of microbial organisms is in fact known to attach and accumulate on the surface of plastic objects, constituting the so-called *plastisphere* (Zettler et al. 2013; Amaral-Zettler et al. 2020; Wright et al. 2020). This community potentially accounts for 1% of the microbial cells in the ocean surface microlayer and up to 1.1×10^4 tons of carbon biomass (Zhao et al. 2021). Biofouling can modify the density properties of initially buoyant microplastic particles, making them prone to sinking (Andrady 2015). Consequently, the motion of biofouled particles also drives a flux of the organic carbon bound to them; furthermore, biofouled microplastic particles may sink faster than natural aggregates that constitute marine snow (Kooi et al. 2017), yet another way in which microplastics could impact the carbon cycle (Galgani and Loiselle 2021; Kvale et al. 2021). Although there is ongoing debate about whether the export at depth of organic particulates may demonstrate the strength of the biological carbon pump or not (*see* Koeve et al. 2020; Nowicki et al. 2022), here we focus on how carbon export is affected by microplastic pollution, as it is indeed an important component of the marine biological pump.

Our work aims at simulating and assessing the occurrence of carbon export mediated by microplastics (assumed here to be 1-mm spheres) in the Mediterranean Sea, and the spatial distribution of the most important areas for such export. Because the Mediterranean has high concentrations of microplastics and is highly exposed to the effects of climate change, the microplastic-mediated carbon export could be particularly relevant here. We use the novel Lagrangian–Eulerian framework elaborated in Guerrini et al. (2022) and the Parcels framework for Lagrangian particle-tracking (Delandmeter and Van Sebille 2019) to model (1) the sinking behavior of prototypical microplastic particles related to biofouling dynamics (following Fischer et al. 2022) at several locations in the Mediterranean Sea and (2) the interaction between the carbon in microplastics' biofilm, the concentrations of dissolved inorganic carbon (DIC), and the particulate organic carbon (POC) in the water column. In order to provide a preliminary potential estimate of how microplastic biofilm development can modify organic carbon fluxes, we test the effects using different scenarios of particle concentrations on the entire Mediterranean basin. We also simulate the carbon export resulting from two realistic scenarios of microplastic pollution in the Mediterranean Sea provided by Everaert et al. (2020), one representing the recent past (2004, which has been regarded as a typical year for the biogeochemical parameters linked to biofouling; *see* Lobelle et al. 2021, and S1 therein) and one for mid-century future (2050) counts of microplastics, where business-as-usual trends in plastic production are assumed.

Methods

Model setup

The vertical motion of biofouled microplastic particles is simulated using the Parcels (version 2.3.0) Lagrangian particle-tracking framework (Delandmeter and Van Sebille 2019). We describe the biofouling process using the version of the Kooi model (Kooi et al. 2017) modified by Fischer et al. (2022), which simulates diatom growth on microplastic particles. The assumption that the biofilm consists mainly of diatoms is corroborated by recent research, identifying diatoms as early colonizers of marine microplastics (Zettler et al. 2013; Amaral-Zettler et al. 2020; Wright et al. 2020), thus suggesting that they significantly contribute to initiating particle settling.

We simulate biofouling, the consequent vertical motion, and the related carbon export by 1-mm microplastic spheres of low-density polyethylene (LDPE: $920 \, \text{kg m}^{-3}$). These characteristics are quite representative of Mediterranean microplastic pollution: it has been observed that the average plastic particle diameter in Mediterranean samplings is around 1 mm (Ruiz-Orejón et al. 2016; Suaria et al. 2016; Güven et al. 2017), and LDPE has been found to be one of the most common plastic polymers found in the ocean globally (Erni-Cassola et al. 2019). Furthermore, Lobelle et al. (2021) found that the sinking behavior of biofouled microplastics is broadly similar for polymer densities ranging between 30 and $1020 \, \text{kg m}^{-3}$. The modeled items thus described will be referred to shortly as "particles."

As we focus on biofouling-induced–vertical motion of microplastic particles within the water column, we omit their horizontal and vertical displacements caused by transport by ocean currents. Particles are released at the center of each oceanographic grid cell with a $1° \times 1°$ resolution of the Mediterranean Sea (5°E–36°W, 30°N–46°N), at 0.6 m depth (the depth of the first layer in NEMO-MEDUSA, detailed in the section below). Each particle is initialized at the onset of sinking, that is, assuming that, upon release, it carries an amount of attached biofilm that makes it neutrally buoyant when compared to local seawater density. Seawater density is technically computed by informing the polyTEOS10-bsq algorithm, included in Parcels, with salinity and temperature data from NEMO-MEDUSA fields. Our model simulates two plausible scenarios of microplastics concentration for 2004 and 2050, respectively, as proposed by Everaert et al. (2020), and for a series of logarithmically spaced concentrations of particles (1, 10, 100, and 1000 particles m^{-2}; hereafter, p. m^{-2}), which are released in a spatially homogeneous manner over the whole Mediterranean Sea. We model the different concentrations by simulating one particle per location while adjusting the cross section of the water column the particle interacts with (e.g., a 0.01 m^{-2} horizontal water column section is used for simulating a concentration of 100 particles per m^{-2}). This algorithmic expedient allows us to dramatically reduce the computational effort required for simulating the highest concentrations. By using this approach, we are implicitly assuming that particles are all identical, so that the equation of their motion is deterministic. Also, we assume that they do not interact with other particles released at the same location.

Modeling microplastics–seawater carbon exchange

In this work, the biofilm growing on microplastics is simply interpreted as a carbon pool. Following Guerrini et al. (2022), we explicitly simulate the interplay between biofilm dynamics and carbon concentrations in the seawater surrounding each particle as sketched in Fig. 1. The simple equation that describes the dynamics of the biofilm (following Fischer et al. 2022) reads as:

$$\frac{dC}{dt} = G_{coll} + G_{grow} - L_{graz} - L_{resp} - L_{nonlin} \qquad (1)$$

where the G terms are gains and the L terms are losses in the biofilm dynamics and are therefore related to an increase or a decrease of carbon, respectively, in the relevant pool in the surrounding water at the particle's depth. More precisely, G_{coll} represents a particle's collision with free-floating diatoms and their consequent colonization; G_{grow} is the growth of the attached diatoms; L_{graz} describes biofilm grazing; L_{resp} is the biofilm loss rate via respiration; and L_{nonlin} represents processes involving biofilm loss that depend on the abundance of diatoms, such as diseases. The data we use to inform those

terms is further detailed in Section S1 of the Supporting Information. As we are interested in the carbon content of the biofilm, the G and L terms in Eq. 1, which is mutuated after eq. 6 in Fischer et al. (2022), are converted from algal cells unit time^{-1} into mgC unit^{-1} time using the median carbon content in diatoms of 2726×10^{-9} mgC algal cell^{-1} (Menden-Deuer and Lessard 2000). As in Fischer et al. (2022), relevant physical and biogeochemical data are retrieved from the NEMO-MEDUSA-2.0 ORCA00083-N06 (hereafter, MEDUSA) outputs (Yool et al. 2013), a global gridded dataset with 1/12° horizontal resolution, 75 unevenly spaced depth layers, and 5-day averaged data. Among the variables included in the MEDUSA dataset, we use temperature (`potemp`, °C), salinity (`salin`, psu), free-floating diatom (`PHD`) and nondiatom (`PHN`) phytoplankton concentrations (in mmolN m^{-3}), microzooplankton (`ZMI`), and mesozooplankton (`ZME`) concentrations (in mmolN m^{-3}), detritus (`DET`, mmolN m^{-3}), the three-dimensional total primary productivity of both diatoms and nondiatoms (`TPP3`, mmolN m^{-3} d^{-3}), and DIC concentration (`DIC`, mmolC m^{-3}) to calculate biofilm growth on particles and the related change in particle buoyancy.

To model the changes caused by the biofouling of microplastics on the ambient carbon pools (as sketched in Fig. 1), the MEDUSA variables related to the biological carbon cycle are modified during the simulation at each particle's geographic coordinates and depth. For instance, collisions between particles and free-floating diatoms resulting in particle colonization (G_{coll}) determine a decrease in the concentration of the free-floating diatom phytoplankton field (`PHD`) and the transfer of the carbon contained in the ambient seawater algae to the particles. Another process that removes carbon from the water column is diatom growth, driven by primary productivity (`TPP3`), and the related carbon fixation (G_{grow}), which in turn modifies the concentration of DIC in seawater. Three processes cause instead carbon to be released from the biofilm on particles to the surrounding seawater: (1) carbon loss due to algal respiration (L_{resp}) in the form of DIC, (2) grazing of biofilm by mesozooplankton (L_{graz}), and (3) processes that depend on the abundance of diatoms and cause their death, such as diseases and viral lysis (L_{nonlin}). We assume that processes (2) and (3) release carbon in the form of POC, which is equivalent to supposing that the diatom carbon ingested by mesozooplankton will entirely return to the water column upon the organisms' death, thus neglecting respiration (which would contribute to DIC instead). No other removal mechanisms are accounted here to act on the carbon content of the diatom biofilm. We thus neglect interactions among biofouled particles (e.g., collisions), between particles and marine organisms (e.g., ingestion by fish), and between particles and the physical component of the water column, that is, we neglect any effects of shear stress on particles and on the attached biofilm. This latter choice is motivated by the sinking velocity of biofouled particles (reaching up to hundreds of meters per day; Long et al. 2015), that is, indeed too low to force diatom detachment (*see* Characklis 1981).
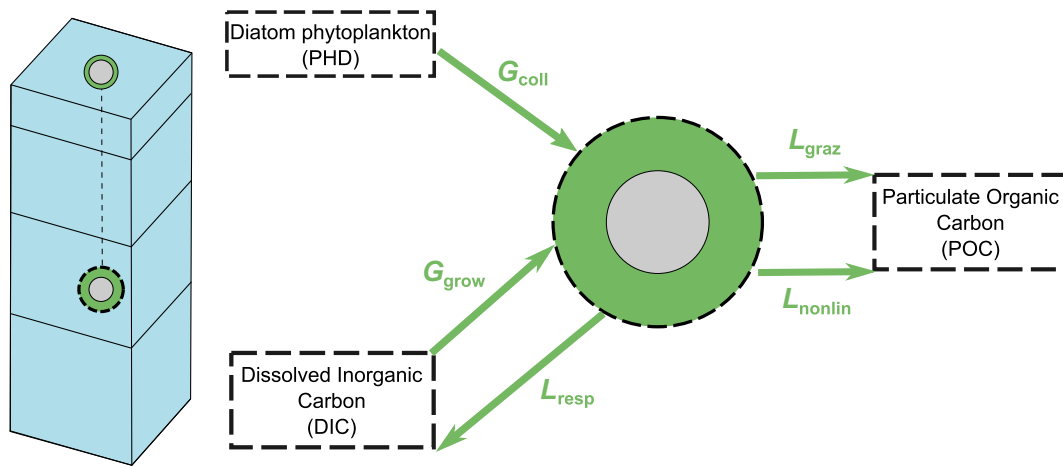
Fig. 1. Schematic representation of the microplastics-seawater carbon exchanges considered in our model. The gray circle is a microplastic particle; the green area surrounding the gray circle represents the biofilm; bold dashed lines contour the carbon pools in our model, namely in the biofilm, free-floating diatom phytoplankton (PHD), POC, DIC, and particle-bound carbon. Green arrows represent the exchanges between the pools, that is, the flow terms of Eq. 1. On the left is a graphical representation of our simulations: a column of water and a neutrally buoyant biofouled microplastic sphere that sinks as the attached biofilm grows.

Note that while the DIC-particle exchanges are two-way, as particles can take up inorganic carbon through biofilm growth (G_{grow}) and then release a fraction of it in the same inorganic form (L_{resp}; *see* Fig. 1), PHD–particle interactions are one-way, meaning that free-floating diatom phytoplankton in the water column can only be depleted, since we neglect the detachment of living diatoms from the particle biofilm. On the other hand, the interaction between particles and the POC field through L_{graz} and L_{nonlin} acts in the opposite direction with respect to the interactions between the particles and the free-floating diatom phytoplankton field, as it can only add organic carbon to the surrounding seawater. Diatom dynamics do not depend on the POC field, but represent instead the only source of POC in this simple model. For this reason, we can assume that the POC field does not require an initial condition prior to the interaction with particles, and thus we initialize it at zero at each depth of the MEDUSA fields.

Figure 2 shows maps of the time-averaged, depth-integrated total primary production (TPP3) for 2004 (Fig. 2) as retrieved from MEDUSA. This variable is of particular relevance for our modeling of biofouling-mediated carbon export, as depth-integrated total primary production can be considered a proxy of diatom growth: thus, its spatial patterns can hint to areas of relevance for microplastics-related carbon export. The depth-integrated total primary production (Fig. 2) shows a steep east-to-west gradient in primary productivity, with the highest values being observed close to the Strait of Gibraltar. Within the generally lower productive Levantine basin of the Mediterranean Sea, there is an area with relatively high primary productivity that is located south of Crete.

In this work, the biogeochemical MEDUSA model is coupled offline with the motion of Lagrangian particles in the water column and with the particle-related updates of carbon tracer fields, as will be detailed below. For the sake of simplicity, we do not feed the particle-modified tracer fields to the MEDUSA model; thus, neither their related modifications are not subject to advection–diffusion processes throughout the water column, nor do these influence the dynamics of other compartments within the MEDUSA model. For these reasons, biofouling-mediated interactions between microplastics and the surrounding seawater cause the carbon and diatom phytoplankton fields in our model to be updated differently with respect to the MEDUSA model at subsequent time steps. Therefore, the length of each run of the simulation is constrained to the time
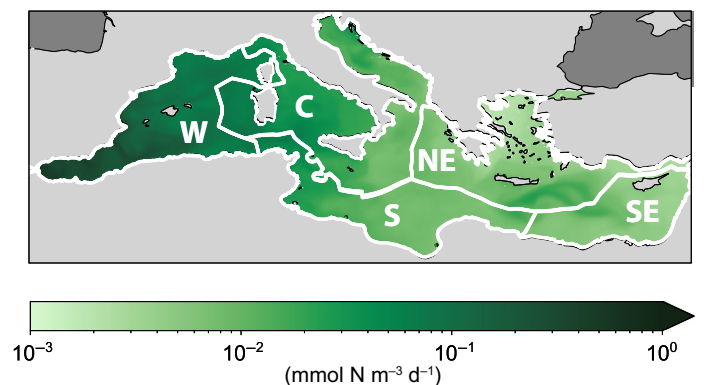

Fig. 2. Time-averaged, depth-integrated maps of total primary production for the year 2004 as obtained from the MEDUSA parameters (TPP3). Overlayed on the map is the partitioning of the Mediterranean Sea in the five regions, as proposed in Guerrini et al. (2022) that will be referenced in the analyses (derived by grouping the maritime boundaries of each of the Mediterranean-facing countries as from the Marine Boundaries v11 product by Flanders Marine Institute 2019). C, central region; NE, northeastern region; S, southern region; SE, southeastern region; W, western region.

resolution of the MEDUSA outputs, that is, 5 d. This relatively short duration of our simulations can still capture the sinking behavior of 1-mm particles effectively because—as emerging from the results by Fischer et al. (2022)—larger microplastics (0.1–1.0 mm) have remarkably shorter oscillation timescales (< 10 d) than smaller fragments (0.01–0.1 mm, up to 130 d). Since there is no full integration of our Eq. 1 within the MEDUSA model that could provide synchronous updating of all the state variables of the problem, we emphasize that the aim of the present work is not to explore any cumulative and/or long-term impacts of microplastics on the biological carbon pump. Rather, we want to assess the potential for the microplastics-mediated pathway to act as an additional carbon export mechanism over timescales relevant to particle sinking due to biofouling.

Vertical profiles of the free-floating diatom phytoplankton (PHD), DIC, and POC fields, acting in our simulations as carbon pools within the water column, are initialized at the beginning of each 5-d simulation using the MEDUSA data of the starting day; their subsequent changes caused by particle interactions are stored at the same time steps as particle data. PHD and DIC are stored with their original units (namely, $mmolN\,m^{-3}$ and $mmolC\,m^{-3}$), while the POC field is in $mgC\,m^{-3}$. Following Guyennon et al. (2015), we consider the POC that is found below 100 m depth as being "exported."

To set the contribution of biofouled microplastics apart from that of a natural biological carbon export scenario, we test the interplay between the different surface concentrations of particles and the environmental conditions of a typical year, thus removing the confounding factor of interannual differences in the meteorological forcings. Starting from each given particle concentration, particle–seawater carbon interactions are simulated for 12 months, from December 2003 to November 2004. The 5-d averaged MEDUSA data are used to set the initial conditions for each 5-d run of our simulations: by doing so, our simulations account for the different nutrient concentrations and temperature profiles across the Mediterranean Sea and their seasonal variations. The vertical position, biofouling state, and field carbon concentrations are updated using a 4th-order Runge–Kutta method with an integration time step of 60 s and stored every 3 h of simulation. Longer integration time steps were tested and caused a poorer description of particles' sinking trajectories, especially in case of vertical oscillations in the particles' trajectories. Oscillatory patterns frequently arise due to the interplay of the attached organisms' dynamics, their response to environmental variables, particle characteristics, and density gradients in the water column (Kooi et al. 2017; Kreczak et al. 2021; Lobelle et al. 2021). Our modeling results of microplastics-mediated carbon export are lastly compared with POC export calculated by Guyennon et al. (2015), who time-averaged a 15-yr (1998–2012) simulation of the hydrodynamics and biogeochemistry of the Mediterranean Sea.
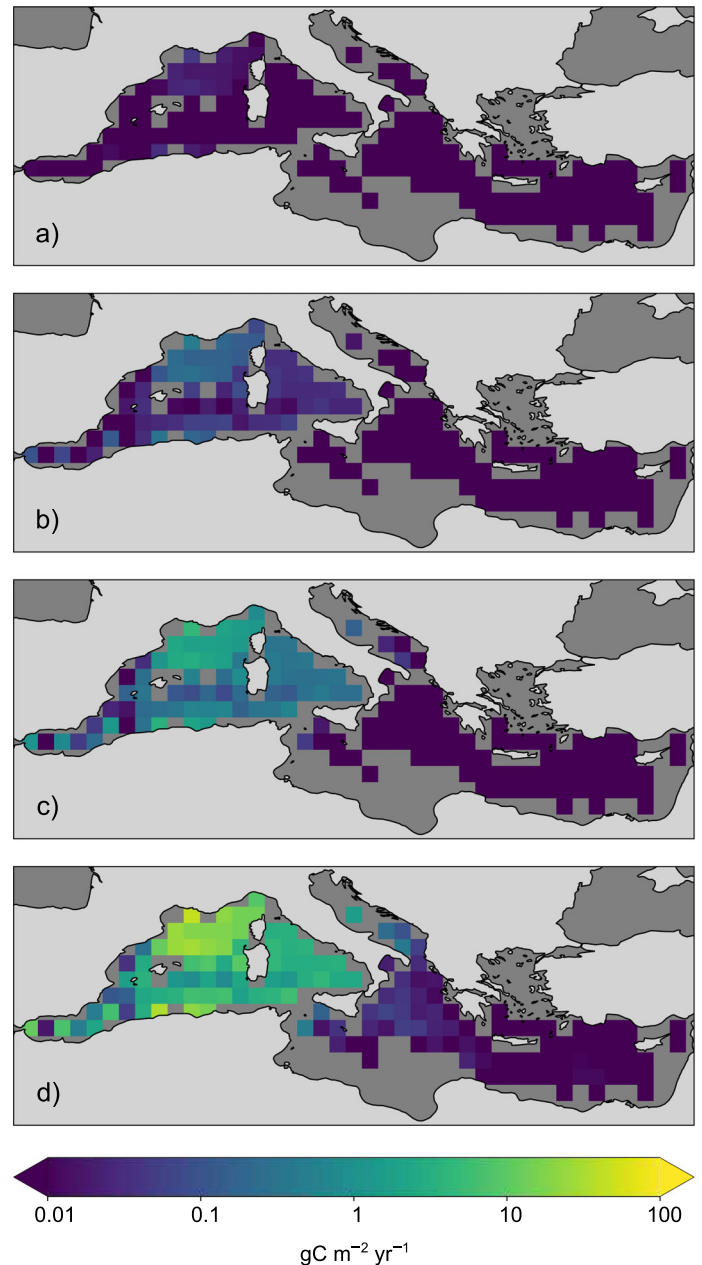

Fig. 3. Estimates of yearly particle-mediated carbon export below 100 m depth (in $gC\,m^{-2}yr^{-1}$) for the four surface microplastic concentrations tested. (**a**) 1 p. m^{-2}; (**b**) 10 p. m^{-2}; (**c**) 100 p. m^{-2}; (**d**) 1000 p. m^{-2}.

Results

Yearly maps with estimations of carbon export below 100 m depth caused by 1-mm microplastics biofouled by diatoms are shown in Fig. 3 for the different tested surface log-scaled concentrations (from 1 to 1000 p. m^{-2}). At all concentrations, particle-mediated carbon export appears to be more intense in the western part of the Mediterranean basin, which is also an area characterized by high total primary productivity (*see* Fig. 2 where the Mediterranean regions are also defined)

and thus more favorable for diatom growth. No export below 100 m depth seems to occur in the Southern Mediterranean Sea in any of our simulations, due to the shallower sinking depths reached by particles released there (*see* Fig. S1 in the Supporting Information). Particle concentration is also clearly correlated to the particle-mediated carbon export below 100 m: at the lowest surface concentrations (i.e., 1 and 10 p. m^{-2}), little POC (< 1 gC m^{-2} yr^{-1}) is released at depth, with a slight increase in some highly productive areas in the Northwestern Mediterranean Sea. Particle-mediated export is also relatively high in the central region of the basin for particle concentrations from 100 p. m^{-2}.

The monthly averaged daily export rates per particle (in mgC p.$^{-1}$ d.$^{-1}$) are shown in Fig. 4 for each of the four simulated concentrations of microplastics, also unraveling their spatial patterns over the five Mediterranean regions shown previously in Fig. 2 (*see* the Supporting Information for details). Seasonality seems to play an important role in particle-mediated carbon export—winter (December–February) and spring (March–May) are characterized by the strongest export fluxes, if any. In fact, the Western Mediterranean basin (Fig. 4a) is the only area showing particle-mediated carbon export almost all year round, except for the month of July, and the one with the highest average value (about 0.06

mgC p.$^{-1}$ d.$^{-1}$). In the other regions, the particle-mediated carbon export is generally lower (halved in the central region, and about two orders of magnitude lower in the southern, northeastern, and southeastern regions), and limited to winter and spring only. Notably, the southeastern region (Fig. 4e) is where particle-mediated carbon export occurs for the shortest time period, from January to March, corresponding to the phytoplankton bloom in late winter/spring (Sammartino et al. 2015).

Although the concentration of particles typically does not seem to significantly affect particle sinking depth (*see* Fig. S1 in the Supporting Information) and the related daily POC export throughout the year, some exceptions occur in summer. In June, August, and (to a lesser extent) in October, the amount of carbon transported below 100 m by each particle in the western region (Fig. 4a) seems to be higher at the highest particle concentration. Furthermore, the 1000 p. m^{-2} simulation is the only one in which some export occurs also during September, similarly to what happens in the central and southern regions in June (Fig. 4b,c *see* Fig. S1 in the Supporting Information for mapped sinking depths).

The 2004 and 2050 scenarios of microplastic pollution in the Mediterranean Sea (as provided by Everaert et al. 2020) are redrawn in Fig. 5a,b, together with the carbon exports
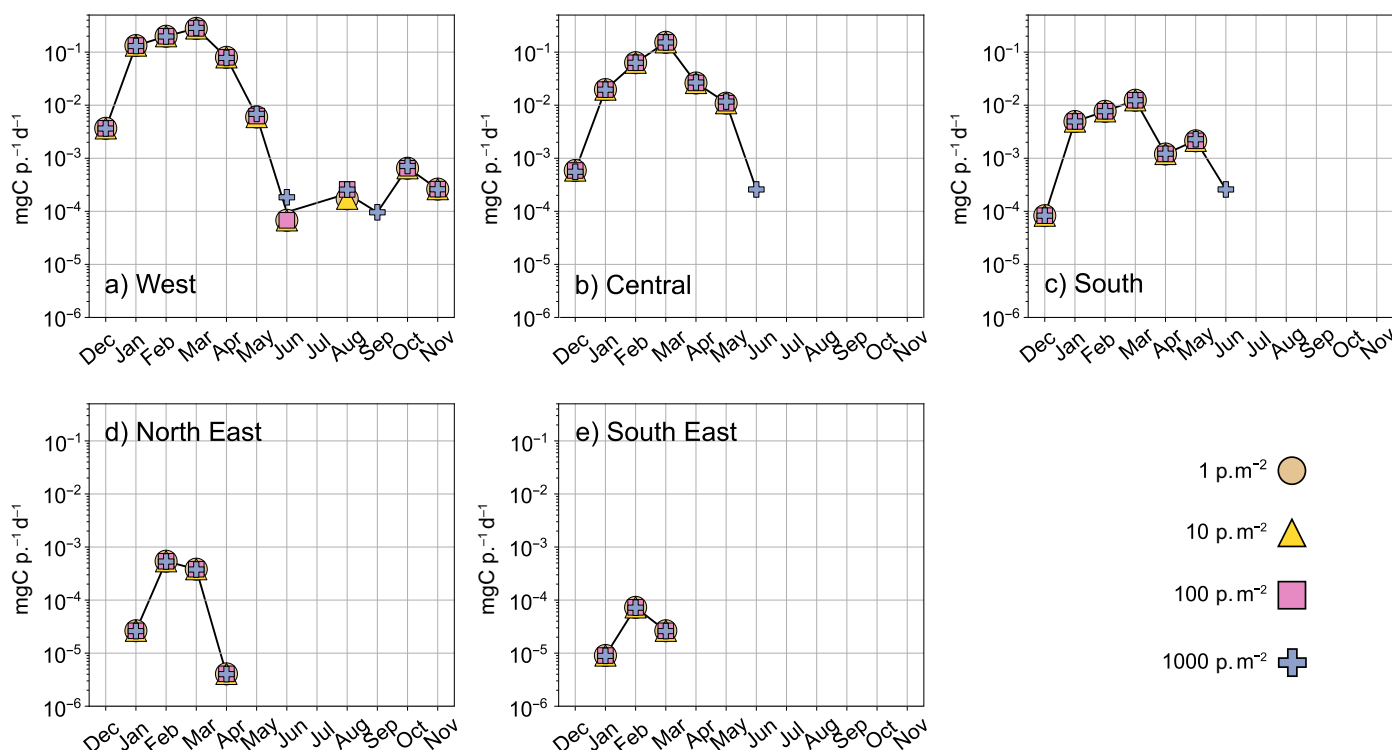

Fig. 4. Amount of carbon exported below 100 m depth during first sinking, per plastic particle per day, across the 1-yr-long simulation for each of the four tested concentrations of microplastics. First sinking is defined as the maximum depth reached by a sinking particle when its sinking velocity (Eq. S1 in the Supporting Information) changes sign due to biofouling-related modifications in buoyancy. Each plot refers to the spatially averaged value in the relative Mediterranean region. Absence of plotted values means that no microplastic-mediated carbon export was registered during that month in our simulations.
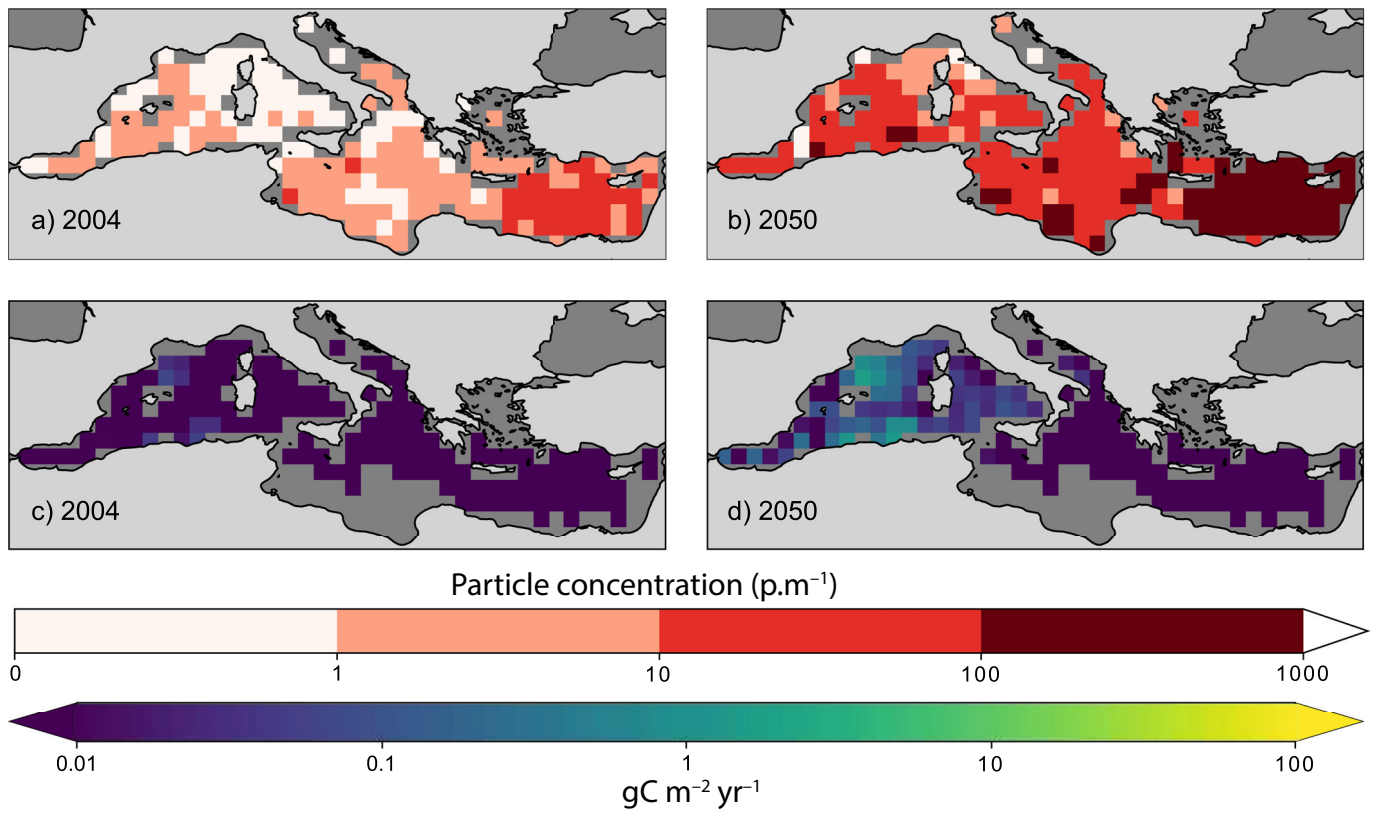
Fig. 5. Particle concentrations and resulting maps of particle-mediated carbon export for the two scenarios of microplastic concentrations of 2004 and 2050. Upper plots: particle concentrations in 2004 (**a**) and 2050 (**b**), redrawn after Everaert et al. (2020). Lower plots: estimates of yearly carbon export (in gC m^{-2}yr^{-1}) below 100 m for 2004 (**c**) and 2050 (**d**).

resulting from our simulations (Fig. 5c,d). It is worth noticing that the particle concentrations used to simulate the 2004 scenario (Fig. 5a) are closer to the lower-concentration scenarios used for the previous simulations (1–100 p. m^{-2}), while the projected microplastics concentrations for 2050 are closer to those of the higher-concentration scenarios (100–1000 p. m^{-2}). Interestingly, although the highest counts of microplastics are found in the eastern part of the basin in both the 2004 and 2050 scenarios, these areas do not seem to contribute to carbon export significantly because primary productivity is much lower there. In fact for year 2004 (Fig. 5c), microplastics-mediated carbon export is expected only in few locations of the Western region, namely between the Spanish Balearic Islands and the French Gulf of Lion, and along the Algerian coasts, and with very low values (around 0.1 gC m^{-2} d^{-1}). The same areas yield higher carbon export if polluted with the concentrations of microplastics projected for 2050 (Fig. 5d), with particle-mediated carbon export above 0.1 gC m^{-2} d^{-1} in most of the western region and part of the central one, up to the Italian coasts.

A comparison between our estimates of yearly carbon export in each of the five Mediterranean regions for the 2004 and the 2050 plastic pollution scenarios and the estimates of biological carbon export produced by Guyennon et al. (2015;

see Fig. 5) are reported in our Fig. 6. As also suggested by Fig. 5c,d, the areas with lower total primary production, such as the southern, the northeastern, and the southeastern regions seem to be those where carbon export due to sinking microplastic particles could contribute less to biological carbon export. The expected share of biological carbon export that can be ascribed to particles amounts to < 1% in all regions for the 2004 scenario, with a Mediterranean-wide average of 0.07%. However, at 2050 concentrations, particle-mediated carbon export could start representing a pathway for carbon export in the western (4.5% of the total yearly POC export) and central (2.8%) regions.

Discussion

Our results outline that microplastics-mediated carbon export depends not only on local microplastics concentrations but also on geographic and on seasonal factors. In fact, it is mainly confined to the western and central regions of the Mediterranean Sea in winter and spring, with the eastern regions presenting a negligible contribution to this phenomenon. These regional and seasonal variations in microplastic-mediated carbon export in our results are caused by an interplay between regional density gradients, both longitudinally
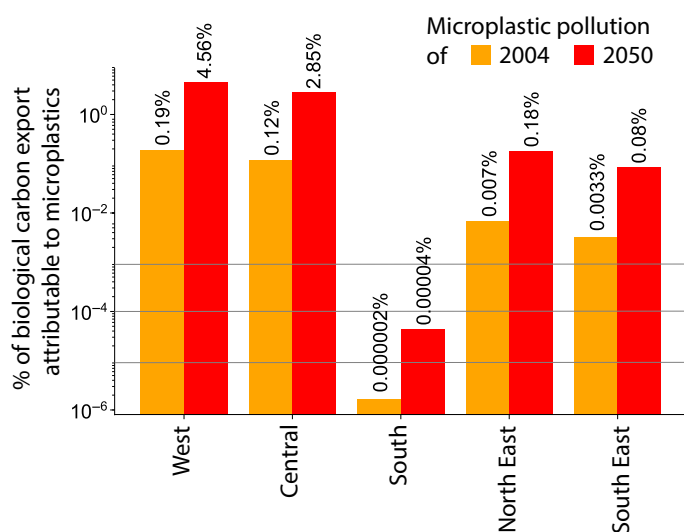
Fig. 6. Fraction of the total yearly POC export below 100 m, as obtained feeding our model with the data by Guyennon et al. (2015), that can be attributed to microplastic particles in each of the five regions of the Mediterranean Sea.

and throughout the water column, and different biofilm growth/decay patterns caused by local temperature, mixed layer depth, nutrient availability, and the related total primary productivity, that are related to seasonal patterns. In particular, the Mediterranean Sea is characterized by a strong west-to-east gradient in nutrient concentrations, with the Eastern Mediterranean Sea being characterized by ultraoligotrophic properties (Lazzari et al. 2016), hampering primary productivity in those areas. Furthermore, the eastern regions tend to be more saline, and thus denser, than western regions (*see*, for instance, among others, the recent work by Sammartino et al. 2022), hindering the sinking of biofouled microplastic particles there and the related carbon export. The spatiotemporal patterns of carbon export projected in the present study are coherent with those obtained by Guyennon et al. (2015) using a microplastics-free full account of the Mediterranean biogeochemistry and hydrodynamics, as well as with the measurements taken by Kessouri et al. (2018) in the western region. This agreement between the spatial and seasonal patterns of carbon export caused by either microplastics-mediated mechanisms or the biological carbon pump pathways intuitively suggests that the areas of the Mediterranean basin where the biological carbon export is more intense are also of primary interest when examining how this mechanism can be affected by microplastic pollution.

The carbon export related to the 2004 plastic pollution scenario is small compared to the overall magnitude of the estimated biological carbon export in the Mediterranean Sea (Fig. 6). This is also the case for the 1–10 p. m^{-2} simulations, for which the surface microplastics concentrations used as inputs are similar to those of the 2004 scenario (compare

Fig. 3a,b with Fig. 5c). However, current trends in concentrations of microplastics related to business-as-usual plastic input to the Mediterranean Sea (Everaert et al. 2020) could start impacting carbon export in the western and central regions over the next decades. For instance, when our model is run under the expected microplastic pollution scenario of 2050 (Fig. 5b), microplastics-mediated carbon export occurs in the entire western region, and accounts for 4.5% of the total natural POC export there (Fig. 6). Some plastic-mediated export (comprising 2.8% of POC export in the area) is found also in the central region by 2050.

According to projections by Everaert et al. (2020), microplastic concentrations in the Mediterranean Sea will be, on average, 25 times higher in 2050 than in 2004 due to the increase in plastic production and waste. Assuming that nutrient availability will not change significantly, as in the case of our simulation setup, such an increase would be mirrored by an equivalent growth in microplastics-mediated carbon export (as shown in Fig. 6), suggesting a linear relationship between the surface concentration of microplastics- and plastic-mediated carbon export to depth, at least within the range of concentrations we considered. This relationship is in fact apparent in our simulations not only in their yearly carbon export fluxes (Fig. 3), but also—and perhaps even more prominently—when examining daily particle-wise carbon exports (Fig. 4), for which no significant differences were found within the range of tested surface microplastic concentrations. Consequently, in the 100 and 1000 p. m^{-2} scenarios, which represent, for several locations in the Mediterranean Sea, microplastic concentrations higher than those projected for 2050, the fraction of carbon export due to the sinking of biofouled particles is expected to increase remarkably. For instance, in the 100 p. m^{-2} simulation, the western and central regions contribute to about 14% and 19%, respectively, to the yearly POC carbon export there, and even exceed the natural biological export reported by Guyennon et al. (2015) in the 1000 p. m^{-2} simulation.

Microplastics could thus cause unforeseeable effects on the biogeochemistry of the highly productive waters of the western and central regions. Conversely, in less productive areas (like the Levantine basin; *see* Fig. 2), particle-mediated carbon export seems to be absent for most of the year (May to December) and, consequently, to contribute less to the share of carbon export in this region (Fig. 6). Mechanisms other than diatom phytoplankton mortality could be dominating the biological carbon pump in those regions, for example, mortality of other organisms (mesozooplankton and ciliates), the egestion of fecal pellets, and sloppy feeding by mesozooplankton, among those included in the Guyennon et al. (2015) study, or coastal discharge and shelf resuspension, as documented by Alkalay et al. (2019). Moreover, these natural aggregates are generally denser (1.08 g cm^{-3} for marine snow, up to 1.70 g cm^{-3} for fecal pellets, and a median of 1.17 g cm^{-3} for biofouling organisms; *see* Amaral-Zettler

et al. 2021) than negatively buoyant biofouled microplastics, so their sinking below the 100-m mark (thereby contributing to carbon export) is expected to be less affected by seasonal vertical mixing.

The approach presented here is certainly a simplified one. In fact, we simulated the dynamics and interactions of biofouled particles along 5-d-long independent runs, without accounting for advection–diffusion processes affecting the carbon pools through the water column. Such a dynamic that would have required computationally intensive online integration of our module into MEDUSA. Also, our model neglects the possible biogeochemical interactions with other components of the marine carbon pump, for example, other microbial organisms interacting with the ambient POC. Furthermore, our simulations are carried out over a 1×1 grid, thus our model is currently not suitable to capture submesoscale variability in physical and biological variables driving Mediterranean marine productivity (Marrec et al. 2018). We recognize that coupling microplastics-mediated carbon export dynamics with a comprehensive description of the biogeochemistry and hydrodynamics of the Mediterranean Sea, possibly at a finer spatial resolution, is crucially required to assess long-term impacts of microplastics on the biological carbon pump, in particular in relation to changes in temperature and nutrient availability, two aspects that are being consistently affected by climate change. Nevertheless, increasing the resolution of our results would have required to reproduce with a finer scale model the microplastic pollution scenarios offered by Everaert et al. (2020), an effort that goes well beyond the scope of the present work.

Furthermore, our biofouling model is somewhat simplified, as it accounts only for the dynamics of diatoms among the different organisms of the so called "plastisphere" (Zettler et al. 2013) that can contribute to oceanic carbon fluxes. The microbial community growing on the surface of plastics can in fact develop over time and become very diverse (Amaral-Zettler et al. 2020), also with regional signatures (Amaral-Zettler et al. 2021), and could respond differently to changes in the available nutrients in the water column, thus potentially inducing different particle sinking behaviors in long-term simulations. Future studies should also account for the variety of sizes and shapes of microplastic particles, as these properties can affect both biofouling dynamics and sinking timescales (Karkanorachaki et al. 2021; Lobelle et al. 2021), also considering the potential for biofouled microplastics to oscillate throughout the water column or sink at depths shallower than 100 m in response to biofilm dynamics and density gradients (Kooi et al. 2017). This mechanism requires further attention, as in principle it could prevent the carbon content of the biofilm onto these microplastics from being exported at depth. In addition, sinking plastic particles could be accounted as POC themselves, and be accordingly included in carbon sequestration fluxes (Kharbush et al. 2020; Stubbins et al. 2021). It is possible to compare the carbon export due to the carbon content of microplastic particles with the one

related to the biofilm they carry through a rough calculation. The microplastic particles modeled in our simulations are 1-mm LDPE spheres (density $= 920 \, kg \, m^{-3}$), thus each modeled microplastic weighs 3.85 mg. LDPE has a carbon content of $\sim 80\%$ (as reported, for instance, in Smeaton 2021), yielding 3.08 mgC per microplastic particle. Peak daily carbon export per particle in our models is ~ 0.1 mgC p.$^{-1}$ d^{-1}. This would mean that the ratio exported C : plastic C can almost reach, in our model, at most 1 : 31. Furthermore, extrapolating from our roughly calculated ratio and the estimated yearly sequestration of plastics in ocean depth that accounts for 7.8 ± 1.73 MtC of carbon that globally reaches the seabed every year (Smeaton 2021), the upper bound estimate of the associated carbon export due to the biofouling of such plastics could amount to ~ 0.2 MtC. As stated, this is inherently an overestimate: in fact, not all the plastics reaching the seabed are the same as our modeled microplastic particle in terms of polymer type, shape, and size. For instance, a large fraction in mass of the plastic found on the seabed is made of high-density materials (e.g., the work by Erni-Cassola et al. 2019) that sink rapidly after entering the ocean, hampering the growth of biofilm.

Conclusions

We have provided a first, simplified model for carbon export mediated by the sinking of biofouled microplastics in the Mediterranean Sea elaborating over the framework of seawater–particle exchange developed by Guerrini et al. (2022). We simulated an array of surface concentrations of virtual microplastic particles within a Lagrangian framework, as well as their colonization by diatoms and consequent vertical movements in the water column, using the biofouling model proposed by Fischer et al. (2022). Upon sinking, particles interact with carbon pools in the water column (namely, free-floating diatom phytoplankton, DIC, and POC) via the dynamics of the biofilm, thereby contributing to biological carbon export. Our simulations provide a preliminary estimation of the magnitude of microplastics-mediated carbon export in the Mediterranean Sea. Results show that biofouled microplastics may contribute to a small fraction of the baseline biological carbon export below 100 m depth in the Mediterranean Sea. Particle-mediated carbon export is highest in the western and central areas of the basin, and peaks in the early spring season. Comparing our outcomes with Mediterranean-wide studies (Guyennon et al. 2015) and local sampling campaigns (Kessouri et al. 2018), we find that the spatial and temporal patterns we detected in microplastics-mediated carbon export mirror those related to the natural biological carbon pump, suggesting that the sinking of biofouled particles could act as an additional export mechanism.

Nonetheless, given the series of assumptions underlying the simplified model, it is still challenging to infer whether

the contribution of microplastics could increase the natural biological carbon export, and if any increase would in turn impact marine ecosystems. For instance, the modeling approach proposed by Kvale et al. (2021) showed that the reduced grazing of phytoplankton, caused by zooplankton feeding instead on microplastics, could cause an increase in the sinking of phytoplankton as detritus globally, which in turn would deplete oxygen at depth upon remineralization (Kvale et al. 2021), potentially exacerbating hypoxia in some regions. The complexity and variety of the mechanisms contributing to the marine carbon cycle, and their interplay, need to be considered in a holistic manner. Further modeling experiments that couple particle-based approaches with a comprehensive description of the underlying biogeochemistry and hydrodynamics of the Mediterranean Sea, including a wider variety of plastic particle sizes, shapes, and densities (Kooi and Koelmans 2019), and considering anthropogenic inputs and current-driven dispersal, are thus needed. Interestingly, our results for the 2050 scenario of microplastic pollution suggest that the contribution of microplastic-mediated carbon export on the biological carbon pump could increase in the future; in this respect, more in-depth analyses, including simulations over longer time horizons, might be crucial to increase the knowledge on this phenomenon. This perspective is also supported by recent research suggesting that plastics could impact on biological carbon pumping at centennial or longer timescales (Kvale 2022). Future climate scenarios also need to be included in modeling efforts in this line of research, as the Mediterranean Sea is warming 25% faster than the global mean (Cramer et al. 2018). By the end of the century, according to the models of the MED-CORDEX ensemble ranging between RCP8.5, RCP4.5, and RCP2.6 (Soto-Navarro et al. 2020), the Mediterranean Sea is expected to be subject to a temperature increase of 0.81–3.71°C in the first 150 m of depth, as well as a reduction of the nutrients in the basin, and the consequent decrease (up to 20%) in the rate of carbon export at 1000 m, especially in the Western Mediterranean (Pagès et al. 2020).

With the presented model, we chose to focus on the Mediterranean Sea, a highly polluted basin with large concentrations of microplastics that could hint at the fate of other areas of the global ocean with similar oceanographic features, like pronounced seasonal stratification and generally oligotrophic waters (*see*, e.g., Moutin and Raimbault 2002). However, our model could be applied to other regional or global scales, including for example tropical upwelling systems, to analyze the relevance of microplastics-mediated pathways within the biological carbon cycle in different contexts. A healthy ocean is key for nature-based measures to tackle the climate crisis, and anthropogenic disturbances represent novel variables in a complex system whose inner interactions are extremely difficult to decipher. For this reason, our study could be the beginning of a research program into understanding the effects of microplastics on the carbon uptake capability of the global ocean and the related impacts on Earth's climate.

Data availability statement

The datasets generated during the study are based on model simulations that use as inputs the biogeochemical data from NEMO-MEDUSA-2.0, and scenarios of plastic concentrations in 2004 and in 2050 after Everaert et al. (2020). The outputs resulting from the current study are available from the corresponding author on reasonable request.

References

Alkalay, R., O. Zlatkin, T. Katz, B. Herut, and I. Berman-Frank. 2019. Mechanisms of C export in the deep South-Eastern Levantine Basin. Rapp. Comm. Int. Mer Medit. **42**: 2019.

Amaral-Zettler, L. A., E. R. Zettler, and T. J. Mincer. 2020. Ecology of the plastisphere. Nat. Rev. Microbiol. **18**: 139–151. doi:10.1038/s41579-019-0308-0

Amaral-Zettler, L. A., and others. 2021. Diversity and predicted inter- and intra-domain interactions in the Mediterranean Plastisphere. Environ. Pollut. **286**: 117439. doi:10.1016/j.envpol.2021.117439

Andrady, A. L. 2015. Persistence of plastic litter in the oceans, p. 57–72. *In* M. Bergmann, L. Gutow, and M. Klages [eds.], Marine anthropogenic litter. Springer Int. Publishing.

Characklis, W. G. 1981. Bioengineering report: Fouling biofilm development: A process analysis. Biotechnol. Bioeng. **23**: 1923–1960. doi:10.1002/bit.260230902

Chen, C. S., C. Le, M. H. Chiu, and W. C. Chin. 2018. The impact of nanoplastics on marine dissolved organic matter assembly. Sci. Total Environ. **634**: 316–320.

Cole, M., P. Lindeque, E. Fileman, C. Halsband, and T. S. Galloway. 2015. The impact of polystyrene microplastics on feeding, function and fecundity in the marine copepod *Calanus helgolandicus*. Environ. Sci. Technol. **49**: 1130–1137. doi:10.1021/es504525u

Cole, M., P. K. Lindeque, E. Fileman, J. Clark, C. Lewis, C. Halsband, and T. S. Galloway. 2016. Microplastics alter the properties and sinking rates of zooplankton faecal pellets. Environ. Sci. Technol. **50**: 3239–3246. doi:10.1021/acs.est.5b05905

Coll, M., and others. 2010. The biodiversity of the Mediterranean Sea: Estimates, patterns, and threats. PLoS One **5**: e11842. doi:10.1371/journal.pone.0011842

Cózar, A., and others. 2014. Plastic debris in the open ocean. Proc. Natl. Acad. Sci. U. S. A. **111**: 10239–10244. doi:10.1073/pnas.1314705111

Cramer, W., and others. 2018. Climate change and interconnected risks to sustainable development in the Mediterranean. Nat. Clim. Change **8**: 972–980. doi:10.1038/s41558-018-0299-2

Delandmeter, P., and E. Van Sebille. 2019. The Parcels v2.0 Lagrangian framework: New field interpolation schemes.

Geosci. Model Dev. **12**: 3571–3584. doi:10.5194/gmd-12-3571-2019

Egger, M., F. Sulu-Gambari, and L. Lebreton. 2020. First evidence of plastic fallout from the North Pacific Garbage Patch. Sci. Rep. **10**: 1–10.

Eriksen, M., and others. 2014. Plastic pollution in the World's oceans: More than 5 trillion plastic pieces weighing over 250,000 tons afloat at sea. PLoS One **9**: 1–15.

Erni-Cassola, G., V. Zadjelovic, M. I. Gibson, and J. A. Christie-Oleza. 2019. Distribution of plastic polymer types in the marine environment; a meta-analysis. J. Hazard. Mater. **369**: 691–698. doi:10.1016/j.jhazmat.2019.02.067

Everaert, G., and others. 2020. Risks of floating microplastic in the global ocean. Environ. Pollut. **267**: 115499. doi:10.1016/j.envpol.2020.115499

Falkowski, P. G., E. A. Laws, R. T. Barber, and J. W. Murray. 2003. Phytoplankton and their role in primary, new, and export production. In: Fasham, M. J. R. (Eds.), Ocean Biogeochemistry. Global Change - The IGBP Series (closed). Springer.

Fischer, R., and others. 2022. Modelling submerged biofouled microplastics and their vertical trajectories. Biogeosciences **19**: 2211–2234. doi:10.5194/bg-19-2211-2022

Flanders Marine Institute. 2019. Maritime boundaries geodatabase: Maritime boundaries and exclusive economic zones (200NM), version 11. Flanders Marine Institute. doi:10.14284/386. Available from https://www.marineregions.org/

Galgani, L., and S. A. Loiselle. 2021. Plastic pollution impacts on marine carbon biogeochemistry. Environ. Pollut. **268**: 115598. doi:10.1016/j.envpol.2020.115598

Giorgi, F. 2006. Climate change hot-spots. Geophys. Res. Lett. **33**: 1–4.

Guerrini, F., L. Mari, and R. Casagrandi. 2022. A coupled Lagrangian-Eulerian model for microplastics as vectors of contaminants applied to the Mediterranean Sea. Environ. Res. Lett. **17**: 024038. doi:10.1088/1748-9326/ac4fd9

Güven, O., K. Gökdağ, B. Jovanović, and A. E. Kıdeyş. 2017. Microplastic litter composition of the Turkish territorial waters of the Mediterranean Sea, and its occurrence in the gastrointestinal tract of fish. Environ. Pollut. **223**: 286–294. doi:10.1016/j.envpol.2017.01.025

Guyennon, A., and others. 2015. New insights into the organic carbon export in the Mediterranean Sea from 3-D modeling. Biogeosciences **12**: 7025–7046. doi:10.5194/bg-12-7025-2015

Heinze, C., and others. 2019. ESD reviews: Climate feedbacks in the Earth system and prospects for their evaluation. Earth Syst. Dynam. **10**: 379–452. doi:10.5194/esd-10-379-2019

Karkanorachaki, K., E. Syranidou, and N. Kalogerakis. 2021. Sinking characteristics of microplastics in the marine environment. Sci. Total Environ. **793**: 148526.

Kessouri, F., C. Ulses, C. Estournel, P. Marsaleix, F. D'Ortenzio, T. Severin, V. Taillandier, and P. Conan. 2018. Vertical mixing effects on phytoplankton dynamics and organic carbon export in the Western Mediterranean Sea. J. Geophys. Res. Oceans **123**: 1647–1669. doi:10.1002/2016JC012669

Kharbush, J. J., and others. 2020. Particulate organic carbon deconstructed: Molecular and chemical composition of particulate organic carbon in the ocean. Front. Mar. Sci. **7**: 1–10.

Koeve, W., P. Kähler, and A. Oschlies. 2020. Does export production measure transient changes of the biological carbon pump's feedback to the atmosphere under global warming? Geophys. Res. Lett. **47**: e2020GL089928. doi:10.1029/2020GL089928

Kooi, M., E. H. V. Nes, M. Scheffer, and A. A. Koelmans. 2017. Ups and downs in the ocean: Effects of biofouling on vertical transport of microplastics. Environ. Sci. Technol. **51**: 7963–7971. doi:10.1021/acs.est.6b04702

Kooi, M., and A. A. Koelmans. 2019. Simplifying microplastic via continuous probability distributions for size, shape, and density. Environ. Sci. Technol. Lett. **6**: 551–557. doi:10.1021/acs.estlett.9b00379

Kreczak, H., A. J. Willmott, and A. W. Baggaley. 2021. Subsurface dynamics of buoyant microplastics subject to algal biofouling. Limnol. Oceanogr. **66**: 1–13.

Kvale, K. 2022. Implications of plastic pollution on global marine carbon cycling and climate. Emerg. Top. Life Sci. **6**: 359–369. doi:10.1042/ETLS20220013

Kvale, K. F., A. E. Friederike Prowe, and A. Oschlies. 2020a. A critical examination of the role of marine snow and zooplankton fecal pellets in removing ocean surface microplastic. Front. Mar. Sci. **6**: 1–8.

Kvale, K. F., A. E. F. Prowe, C.-T. Chien, A. Landolfi, and A. Oschlies. 2020b. The global biological microplastic particle sink. Sci. Rep. **10**: 1–12.

Kvale, K. F., A. E. F. Prowe, C.-T. Chien, A. Landolfi, and A. Oschlies. 2021. Zooplankton grazing of microplastic can accelerate global loss of ocean oxygen. Nat. Commun. **12**: 2358.

Laufkötter, C., and others. 2016. Projected decreases in future marine export production: The role of the carbon flux through the upper ocean ecosystem. Biogeosciences **13**: 4023–4047. doi:10.5194/bg-13-4023-2016

Lazzari, P., C. Solidoro, S. Salon, and G. Bolzon. 2016. Spatial variability of phosphate and nitrate in the mediterranean sea: A modeling approach. Deep Sea Res. Part I Oceanogr. Res. Pap. **108**: 39–52. doi:10.1016/j.dsr.2015.12.006

Lejeusne, C., P. Chevaldonné, C. Pergent-Martini, C. F. Boudouresque, and T. Pérez. 2010. Climate change effects on a miniature ocean: The highly diverse, highly impacted Mediterranean Sea. Trends Ecol. Evol. **25**: 250–260. doi:10.1016/j.tree.2009.10.009

Lobelle, D., M. Kooi, A. A. Koelmans, C. Laufkötter, C. E. Jongedijk, C. Kehl, and E. van Sebille. 2021. Global modeled sinking characteristics of biofouled microplastic.

J. Geophys. Res. Oceans **126**: e2020JC017098. doi:10.1029/2020JC017098

Long, M., B. Moriceau, M. Gallinari, C. Lambert, A. Huvet, J. Raffray, and P. Soudant. 2015. Interactions between microplastics and phytoplankton aggregates: Impact on their respective fates. Mar. Chem. **175**: 39–46. doi:10.1016/j.marchem.2015.04.003

Marrec, P., and others. 2018. Coupling physics and biogeochemistry thanks to high-resolution observations of the phytoplankton community structure in the northwestern Mediterranean Sea. Biogeosciences **15**: 1579–1606. doi:10.5194/bg-15-1579-2018

McGinty, N., A. M. Power, and M. P. Johnson. 2011. Variation among northeast Atlantic regions in the responses of zooplankton to climate change: Not all areas follow the same path. J. Exp. Mar. Biol. Ecol. **400**: 120–131. doi:10.1016/j.jembe.2011.02.013

Menden-Deuer, S., and E. J. Lessard. 2000. Carbon to volume relationships for dinoflagellates, diatoms, and other protist plankton. Limnol. Oceanogr. **45**: 569–579. doi:10.4319/lo.2000.45.3.0569

Micheli, F., and others. 2013. Cumulative human impacts on Mediterranean and Black Sea marine ecosystems: Assessing current pressures and opportunities. PLoS One **8**: e79889. doi:10.1371/journal.pone.0079889

Moutin, T., and P. Raimbault. 2002. Primary production, carbon export and nutrients availability in western and eastern Mediterranean Sea in early summer 1996 (MINOS cruise). J. Mar. Syst. **33–34**: 273–288.

Nguyen, T. H., F. H. Tang, and F. Maggi. 2020. Sinking of microbial-associated microplastics in natural waters. PLoS One **15**: 1–20.

Nowicki, M., T. DeVries, and D. A. Siegel. 2022. Quantifying the carbon export and sequestration pathways of the ocean's biological carbon pump. Global Biogeochem. Cycl. **36**: e2021GB007083. doi:10.1029/2021GB007083

Pagès, R., M. Baklouti, N. Barrier, M. Ayache, F. Sevault, S. Somot, and T. Moutin. 2020. Projected effects of climate-induced changes in hydrodynamics on the biogeochemistry of the Mediterranean sea under the rcp 8.5 regional climate scenario. Front. Mar. Sci. **7**: 957.

Passow, U., and C. A. Carlson. 2012. The biological pump in a high CO_2 world. Mar. Ecol. Prog. Ser. **470**: 249–271.

Porter, A., B. P. Lyons, T. S. Galloway, and C. Lewis. 2018. Role of marine snows in microplastic fate and bioavailability. Environ. Sci. Technol. **52**: 7111–7119. doi:10.1021/acs.est.8b01000

Ruiz-Orejón, L. F., R. Sardá, and J. Ramis-Pujol. 2016. Floating plastic debris in the Central and Western Mediterranean Sea. Mar. Environ. Res. **120**: 136–144. doi:10.1016/j.marenvres.2016.08.001

Sammartino, M., A. Di Cicco, S. Marullo, and R. Santoleri. 2015. Spatio-temporal variability of micro-, nano- and pico-phytoplankton in the Mediterranean sea from satellite ocean colour data of seawifs. Ocean Sci. **11**: 759–778. doi:10.5194/os-11-759-2015

Sammartino, M., S. Aronica, R. Santoleri, and B. Buongiorno Nardelli. 2022. Retrieving Mediterranean sea surface salinity distribution and interannual trends from multi-sensor satellite and in situ data. Remote Sens. (Basel) **14**: 2504.

Sjollema, S. B., P. Redondo-Hasselerharm, H. A. Leslie, M. H. Kraak, and A. D. Vethaak. 2016. Do plastic particles affect microalgal photosynthesis and growth? Aquat. Toxicol. **170**: 259–261. doi:10.1016/j.aquatox.2015.12.002

Smeaton, C. 2021. Augmentation of global marine sedimentary carbon storage in the age of plastic. Limnol. Oceanogr. Lett. **6**: 113–118. doi:10.1002/lol2.10187

Soto-Navarro, J., and others. 2020. Evolution of Mediterranean Sea water properties under climate change scenarios in the Med-CORDEX ensemble, v. **54**. Springer.

Stubbins, A., K. L. Law, S. E. Muñoz, T. S. Bianchi, and L. Zhu. 2021. Plastics in the Earth system. Science **373**: 51–55. doi:10.1126/science.abb0354

Suaria, G., and others. 2016. The Mediterranean plastic soup: Synthetic polymers in Mediterranean surface waters. Sci. Rep. **6**: 1–10.

Tetu, S. G., I. Sarker, V. Schrameyer, R. Pickford, L. D. H. Elbourne, L. R. Moore, and I. T. Paulsen. 2019. Plastic leachates impair growth and oxygen production in *Prochlorococcus*, the ocean's most abundant photosynthetic bacteria. Commun. Biol. **2**: 1–9.

The Intergovernmental Panel on Climate Change (IPCC). 2021. Climate change 2021: The physical science basis. Contribution of Working Group I to the Sixth Assessment Report of the Intergovernmental Panel on Climate Change. Technical report.

The Intergovernmental Panel on Climate Change (IPCC). 2022. Climate change 2022: Impacts, adaptation and vulnerability. IPCC.

Troost, T. A., T. Desclaux, H. A. Leslie, M. D. van Der Meulen, and A. D. Vethaak. 2018. Do microplastics affect marine ecosystem productivity? Mar. Pollut. Bull. **135**: 17–29. doi:10.1016/j.marpolbul.2018.05.067

Van Melkebeke, M., C. Janssen, and S. De Meester. 2020. Characteristics and sinking behavior of typical microplastics including the potential effect of biofouling: Implications for remediation. Environ. Sci. Technol. **54**: 8668–8680. doi:10.1021/acs.est.9b07378

Van Sebille, E., and others. 2015. A global inventory of small floating plastic debris. Environ. Res. Lett. **10**: 124006.

Wanninkhof, R., and others. 2013. Global ocean carbon uptake: Magnitude, variability and trends. Biogeosciences **10**: 1983–2000. doi:10.5194/bg-10-1983-2013

Wieczorek, A. M., P. L. Croot, F. Lombard, J. N. Sheahan, and T. K. Doyle. 2019. Microplastic ingestion by gelatinous zooplankton may lower efficiency of the biological pump. Environ. Sci. Technol. **53**: 5387–5395. doi:10.1021/acs.est.8b07174

Wright, R. J., G. Erni-Cassola, V. Zadjelovic, M. Latva, and J. A. Christie-Oleza. 2020. Marine plastic debris: A new surface

for microbial colonization. Environ. Sci. Technol. **54**: 11657–11672. doi:10.1021/acs.est.0c02305

Yool, A., E. E. Popova, and T. R. Anderson. 2013. MEDUSA-2.0: An intermediate complexity biogeochemical model of the marine carbon cycle for climate change and ocean acidification studies. Geosci. Model Dev. **6**: 1767–1811. doi:10.5194/gmd-6-1767-2013

Zettler, E. R., T. J. Mincer, and L. A. Amaral-Zettler. 2013. Life in the "plastisphere": Microbial communities on plastic marine debris. Environ. Sci. Technol. **47**: 7137–7146. doi:10.1021/es401288x

Zhao, S., E. R. Zettler, L. A. Amaral-Zettler, and T. J. Mincer. 2021. Microbial carrying capacity and carbon biomass of plastic marine debris. ISME J. **15**: 67–77. doi:10.1038/s41396-020-00756-2

Conflict of Interest

None declared.